SPRAY CONE ANGLES OF A DUAL PRESSURE SWIRL INJECTOR FOR ATOMIZATION OF ETHANOL AND HYDROGEN PEROXIDE

Gustavo Alexandre Achilles Fischer, fischer@lcp.inpe.br
Fernando de Souza Costa, fernando@lcp.inpe.br
INPE – National Institute for Space Research / Combustion and Propulsion Laboratory
Rodovia Presidente Dutra, km 40, CEP 12.630-000
Cachoeira Paulista/SP - Brazil

Abstract. *The combustion processes in liquid rocket engines are heavily dependent on quality of atomization. Pressure swirl injectors are widely used in liquid rocket engines due to their high efficiency of atomization in a reduced volume. The characteristic geometric parameters of these injectors can be adjusted to control the spray cone angle and improve spray fineness, thus reducing the chamber length and eventual instabilities. A dual pressure swirl injector is characterized by two independent concentric chambers which can provide independent rotational levels to a single or two different liquids to improve mixing and combustion of the propellants within liquid rocket engines. This paper compares theoretical, semiempirical and experimental results concerning the spray cone angles formed by injection of ethanol (C_2H_6O, 95% m/m) and hydrogen peroxide (H_2O_2, 90% m/m) through a dual pressure swirl injector for application in a 100 N bipropellant rocket engine. Data were obtained for injection of water or ethanol through both the primary and secondary chambers and for injection of ethanol in the primary chamber and water through the secondary chamber of the injector. Experimental data are obtained using photographic techniques and are analyzed by image processing software developed in Matlab language.*

Keywords*: Spray Cone Angles, Dual Pressure Swirl Injector, Atomization, Ethanol, Hydrogen Peroxide*

1. INTRODUCTION

The injector is responsible for the atomization of liquid propellants into the combustion chamber of a rocket engine. An efficient atomization allows to significantly increasing the surface area of liquid propellants, ensuring high rates of evaporation, mixing and burning. Small droplets are required to achieve rapid ignition and establish a flame front of the next injection head. The larger droplets take longer to burn and thus define the length of the combustion chamber (Khavkin, 2004).

Ethanol and hydrogen peroxide are green propellants that are being investigated in various research centers and universities (Wernimont, 2006; Maia, 2012; Matos, 2013) due, among other factors, the low environmental impact of combustion, ease of handling and storage, low cost, and good availability on the market. Ethanol and hydrogen peroxide are not hypergolic and therefore require a suitable ignition system or process, for example, auxiliary flames, additives, catalysts, dischargers or heaters.

A pressure swirl injector consists of one or more inlets into a central vortex chamber, the inlets generally being tangential, thus providing the spin in the vortex chamber. Finally the fluid emerges from an orifice in the form of a film around the periphery of the orifice; this film then breaks into a cone of spray droplets. The spray of the liquid produced at the output of this type of injector has the approximate shape of a hollow-cone (Lefebvre, 1989).

A dual pressure swirl injector is characterized by two independent concentric vortex chambers which can provide independent rotational levels to a single liquid or two different liquids. In the case of a dual pressure swirl injector a hollow-cone is formed for each chamber and if the two cones collide there is formation of a single cone. Generally when the cone angle is increased there is also an increase in the contact of droplets of liquid injected with ambient air, which improves the atomization process, the heat and mass transfer. However, the reduction in the cone angle improves the performance of the ignition and extends the limits of stability (Ortmann et al., 1985).

The cone angle is an important external feature of a spray. Due to the interactions of the liquid fuel with air, the spray curve actually has an approximate bell shape, as shown in Fig. 1, thus presenting the difficulty of measuring the cone angle.

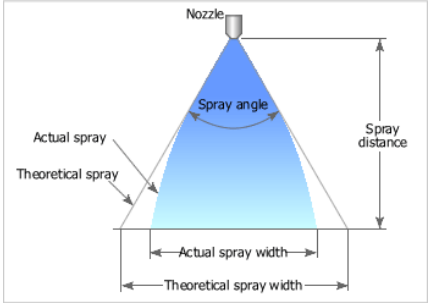

Figure 1. Spray cone angle.

The spray cone angle is the angle α formed by two straight lines in a plane projected from the orifice discharge of injector, at a specified distance (Vásquez, 2011).

This paper compares theoretical, semi-empirical and experimental results concerning the spray cone angles formed by injection of ethanol (C_2H_6O, 95% m/m) and hydrogen peroxide (H_2O_2, 90% m/m) through a dual pressure swirl injector for application in a 100 N bipropellant rocket engine. Data are obtained for injection of water or ethanol through both the primary and secondary chambers and for injection of ethanol in the primary chamber and water through the secondary chamber of the injector. Experimental data are obtained using photographic techniques and are analyzed by image processing software developed in Matlab language by Vásquez (2011).

2. THEORETICAL MODEL

2.1 Ideal model

The theoretical cone angles were calculated using the approach by Abramovich, as described in detail by Fischer (2014). Figure 2 shows a scheme with a pressure swirl injector.

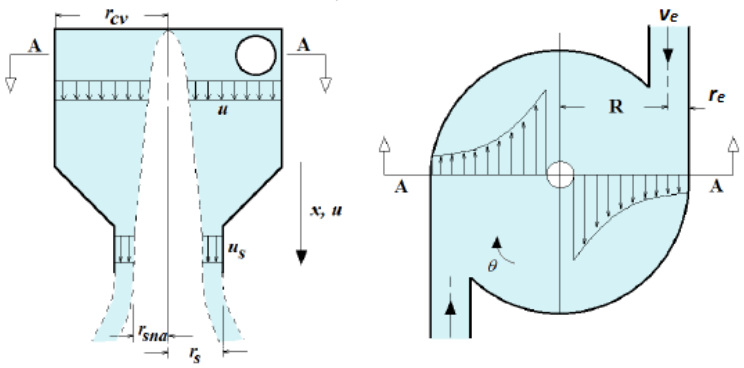

Figure 2. Scheme of a pressure swirl injector.

The characteristic geometric parameter (K) of a pressure swirl injector is defined by:

$$K = \frac{A_s\left(r_{cv} - r_e\right)}{A_e r_s} = \frac{A_s R}{A_e r_s} = \frac{\pi R r_s}{A_e} \tag{1}$$

where A_s is the area and r_s the inner radius of the discharge orifice, A_e is the total area and r_e the radius of tangential inlet channels, r_{cv} is radius and R the effective radius of the vortex chamber.

Other important parameters of the pressure swirl injectors are the liquid fraction area (ε), dimensionless radius of the gas vortex (S), discharge coefficient (μ) and spray cone angle (α). All these parameters are directly related to the K by equations (Bayvel and Orzechowski, 1993):

$$K = \frac{(1-\varepsilon)\sqrt{2}}{\varepsilon\sqrt{\varepsilon}} \tag{2}$$

$$\mu = \varepsilon\sqrt{\frac{\varepsilon}{2-\varepsilon}} \tag{3}$$

$$\tan\frac{\alpha}{2} = \frac{2\mu K}{\sqrt{(1+S)^2 - 4\mu^2 K^2}} \tag{4}$$

$$\mu = \sqrt{1-\mu^2K^2} - S\sqrt{S^2-\mu^2K^2} - \mu^2K^2\ln\left(\frac{1+\sqrt{1-\mu^2K^2}}{S+\sqrt{S^2-\mu^2K^2}}\right) \tag{5}$$

A graphical solution of Eqs. (2), (3), (4) and (5) is shown in Figure 2.

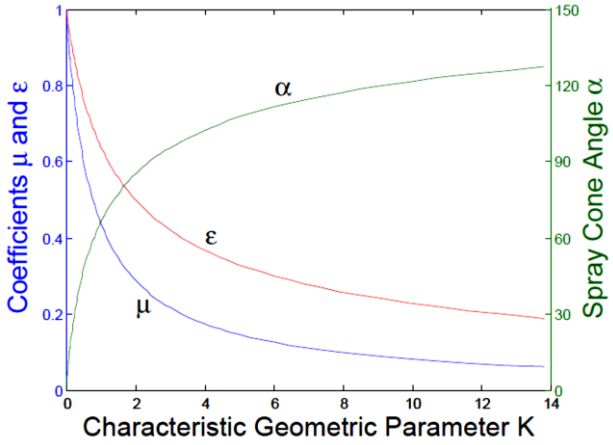

Figure 2. Behavior of the geometric characteristic parameter, discharge coefficient, liquid fraction area and spray cone angle of the pressure swirl injector.

The liquid fraction area (ε) and dimensionless radius of the gas vortex (S) are defined by:

$$\varepsilon = \frac{A_l}{A_s} = \frac{\pi\left(r_s^2 - r_{sna}^2\right)}{\pi r_s^2} = 1 - \frac{r_{sna}^2}{r_s^2} = 1 - S^2 \tag{6}$$

$$S = \frac{r_{sna}}{r_s} = \sqrt{1-\varepsilon} \tag{7}$$

where A_l is the area occupied by liquid and r_{sna} the gas core radius in the discharge orifice.

The spray cone angle in the secondary chamber is derived similarly to the primary chamber, but using the following relation for the characteristic geometrical parameter of the secondary chamber:

$$K_{\sec} = \frac{\pi R_{\sec}\left(r_{\sec}^2 - r_{prim}^2\right)}{A_{e,\sec}\left(r_{\sec} - r_{prim}\right)} \tag{8}$$

where $r_{prim} = r + \delta$ is the external radius and δ is the wall thickness of the discharge orifice of the primary chamber.

2.2 Model considering viscous losses

The theoretical model used here for the flow of viscous liquid into a pressure swirl injector is based on Kliachko approach (Borodin *et al.*, 1967). The characteristic geometric parameter considering the viscous effects (K_λ) must be corrected by equation:

$$K_\lambda = \frac{Rr_s}{\frac{A_e}{\pi} + \left(\frac{\lambda}{2}\right)R\left(R - r_s\right)} = \frac{K}{1 + \left(\frac{\lambda}{2}\right)\left(B^2 - K\right)} \tag{9}$$

where $B = R\sqrt{\pi / A_e}$ and the characteristic geometrical parameter for secondary chamber must be corrected by:

$$K_{\lambda,\sec} = \frac{R_{\sec}\left(r_{\sec}^2 - r_{prim}^2\right)}{\frac{A_{e,\sec}\left(r_{\sec}^2 - r_{prim}^2\right)}{\pi} + \left(\frac{\lambda}{2}\right)R_{\sec}\left(r_{\sec} - r_{prim}\right)\left[R_{\sec} - \left(r_{\sec} - r_{prim}\right)\right]} \tag{10}$$

where the coefficient of friction (λ) is a function of Reynolds number (Re) of the tangential inlet channels obtained from the following equation:

$$\log \lambda = \frac{25{,}8}{\left(\log \mathrm{Re}\right)^{2{,}58}} - 2 \tag{11}$$

Equation (8) for pressure swirl injector is valid for $\mathrm{Re} = 10^3 - 10^5$. The values determined from this equation are significantly higher than from other equations commonly used in hydraulic systems (Bazarov *et al.*, 2004).

Thus, it is possible to recalculate the liquid fraction area (ε_λ) and the dimensionless radius of the gas vortex (S_λ) considering the viscous effects by Eqs. (2) and (7), respectively.

The friction of the liquid on the vortex chamber wall causes a decrease of the angular motion and also energy losses. For a more precise calculation of the pressure drop it is necessary to consider the energy losses in the pressure swirl injector. In the vortex chamber of an injector these losses can be considered as the work of the frictional force on the trajectory of the liquid. Thus, the corrected discharge coefficient (μ_λ) is calculated by:

$$\mu_\lambda = \frac{1}{\sqrt{\dfrac{K_\lambda^2}{1-\varepsilon_\lambda} + \dfrac{1}{\varepsilon_\lambda^2} + \xi_i \dfrac{K^2}{C^2} + \Delta}} \tag{12}$$

where $C = R/r_s$, $\xi = 1/K + \lambda C/2$ and:

$$\Delta = \frac{\lambda}{\xi^2}\left\{\frac{1}{\xi}\left(1-\frac{1}{C}\right) + \lambda\left[\frac{K^2}{4} - \frac{1}{(2\xi-\lambda)^2} + \frac{K}{\xi} - \frac{2}{\xi(2\xi-\lambda)} + \frac{3}{2\xi^2}\ln\left(\frac{(2\xi-\lambda)KC}{2}\right)\right]\right\} \tag{13}$$

The friction coefficient through the tangential inlet channels depends on the Reynolds number (*Re*):

$$\mathrm{Re} = \frac{4\dot{m}}{\pi\mu_l\sqrt{n}d_e} \tag{14}$$

where $\dot{m}$ is the mass flow rate, d_e is the diameter and n the number of tangential inlet channels and μ_l is the dynamic viscosity of the fluid.

The total friction loss in the tangential channels (ξ_i) is computed by:

$$\xi_i = \xi_e + \lambda\frac{l_e}{d_e} \tag{15}$$

where the initial loss coefficient, ξ_e, is determined from Fig. 3, and the inclination of the tangential inlet channels, α_e, is obtained from:

$$\alpha_e = 90^o - \tan^{-1}\left(\frac{r_{cv}}{l_e}\right) \tag{16}$$

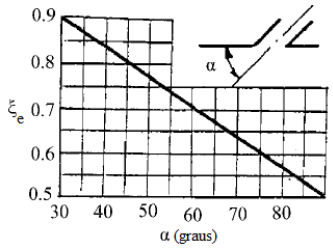

Figure 3. Initial viscous loss coefficient versus inclination of tangential inlet channels.

The corrected spray cone angle (α_λ) is calculated considering the effects of geometry and friction losses:

$$\tan\frac{\alpha_\lambda}{2} = \frac{2\mu_\lambda K_\lambda}{\sqrt{(1+S_\lambda)^2 - 4\mu_\lambda^2 K_\lambda^2}} \tag{17}$$

In the case of a dual pressure swirl injector, the external collision of the two spray cones formed generates another spray cone whose final angle (α_{final}) can be obtained using the momentum conservation equation. Assuming steady flow

conditions, uniform pressure, uniform velocity at the exit orifices and nobody forces give the equilibrium equations in the radial (w) and axial (u) velocity components are:

$$\dot{m}_{prim} w_{prim} + \dot{m}_{\sec} w_{\sec} = \left(\dot{m}_{prim} + \dot{m}_{\sec}\right) w_{final} \tag{18a}$$

$$\dot{m}_{prim} u_{prim} + \dot{m}_{\sec} u_{\sec} = \left(\dot{m}_{prim} + \dot{m}_{\sec}\right) u_{final} \tag{18b}$$

The resulting angle is defined as:

$$\tan\frac{\alpha_{final}}{2} = \frac{w_{final}}{u_{final}} = \frac{\dot{m}_{prim} w_{prim} + \dot{m}_{\sec} w_{\sec}}{\dot{m}_{prim} u_{prim} + \dot{m}_{\sec} u_{\sec}} \tag{18}$$

and it can be written as function of cone semi-angles of inner chamber, α_{prim}, and external chamber, α_{sec}:

$$\tan\frac{\alpha_{final}}{2} = \frac{w_{final}}{u_{final}} = \frac{\dot{m}_{prim} V_{prim} sen\frac{\alpha_{prim}}{2} + \dot{m}_{\sec} V_{\sec} sen\frac{\alpha_{\sec}}{2}}{\dot{m}_{prim} V_{prim}\cos\frac{\alpha_{prim}}{2} + \dot{m}_{\sec} V_{\sec}\cos\frac{\alpha_{\sec}}{2}} \tag{19}$$

where $V = \sqrt{2\Delta P/\rho}$ is the total injection velocity, ΔP the pressure drop in the injector and ρ the density of the fluid.

2.3 Semi-empirical models

Rizk and Lefebvre (Lefebvre, 1989) considered the effects of liquid properties, geometrical parameters, and injection pressure on the liquid film thickness, and derived the following equation for the spray angle:

$$\frac{\alpha}{2} = 6K^{0,15}\left(\frac{\Delta P d_s^2 \rho}{\mu_l^2}\right)^{0,11} \tag{20}$$

Benjamin (1998) validated an equation using a database and modified the coefficients indicated by Rizk and Lefebvre (Lefebvre, 1989) for large size injectors and obtained:

$$\frac{\alpha}{2} = 9.75K^{0,287}\left(\frac{\Delta P d_s^2 \rho}{\mu_l^2}\right)^{0,067} \tag{21}$$

3. EXPERIMENTAL METODOLOGY

3.1 The dual pressure swirl injector

Table 1 shows a general overview of the dual pressure swirl injector dimensions.

Tables 2 and 3 present a general overview of the operational and geometric parameters for design of the primary and secondary chambers of the dual pressure swirl injector, respectively.

Figure 4 show a picture of the manufactured injector.

Table 1. General overview of the dual pressure swirl injector dimensions.

Injector dimensions	Inner	External
Diameter of the discharge orifice – d_s (mm)	1,6	5,2
Length of the discharge orifice – l_s (mm)	8,1	1,4
Number of the tangential inlet channels – n	2	4
Diameter of the tangential inlet channels – d_e (mm)	1,4	2,1
Length of the tangential inlet channels – l_e (mm)	2,8	4,3
Effective radius of the vortex chamber – R (mm)	3,3	4,9
Diameter of the vortex chamber – D_{cv} (mm)	8	12
Length of the vortex chamber – L_{cv} (mm)	4,2	4,6
Transient cone angle – β (º)	90	90

Table 2. General overview of the characteristics of the primary chamber of the dual pressure swirl injector.

Input data				
Pressure drop – ΔP (MPa)			0,2533	
Mass flow rate – $\dot{m}$ (g/s)			10,0538	
Spray cone angle – α (º)			90	
Work fluid			Ethanol	Water
Dynamic viscosity – μ_l (cP)			1,2	1
Density – ρ (kg/m³)			809,3	1000
Injector parameters				
	No viscosity		With viscosity	
Work fluid	Ethanol	Water	Ethanol	Water
Friction coefficient (λ)	0	0	0,073	0,0638
Reynolds number (Re)	0	0	5391,8	6821,6
Spray cone angle – α (º)	90	90	82,2085	83,1008
Discharge coefficient (μ)	0,2226	0,2226	0,264	0,2591
Liquid fraction area (ε)	0,4271	0,4271	0,4808	0,4747
Characteristic geometrical parameter (K)	2,9028	2,9028	2,2028	2,2714
Dimensionless radius of the gas vortex (S)	0,8272	0,8272	0,7689	0,7747
Total injection velocity – V (m/s)	5,5683	5,0093	6,6042	5,8321
Mass flow rate – $\dot{m}$ (g/s)	10,0538	10,0538	11,9241	11,7052

Table 3. General overview of the characteristics of the secondary chamber of the dual pressure swirl injector.

Input data				
Pressure drop – ΔP (MPa)			0,2533	
Mass flow rate – $\dot{m}$ (g/s)			40,2152	
Spray cone angle – α (º)			114,4947	
Work fluid			H_2O_2	Water
Dynamic viscosity – μ_l (cP)			1,13	1
Density (kg/m³)			1405	1000
Injector parameters				
	No viscosity		With viscosity	
Work fluid	H_2O_2	Water	H_2O_2	Water
Friction coefficient (λ)	0	0	0,0509	0,0482
Reynolds number (Re)	0	0	10784	12191
Spray cone angle – α (º)	100,3327	100,3327	95,6415	95,8026
Discharge coefficient (μ)	0,155	0,155	0,1649	0,1643
Liquid fraction area (ε)	0,3415	0,3415	0,3595	0,3585
Characteristic geometrical parameter (K)	4,6667	4,6667	4,2033	4,2254
Dimensionless radius of the gas vortex (S)	0,8834	0,8834	0,8708	0,8714
Total injection velocity – V (m/s)	2,9425	3,4878	3,1315	3,6985
Mass flow rate – $\dot{m}$ (g/s)	40,2152	40,2152	48,0543	48,8002

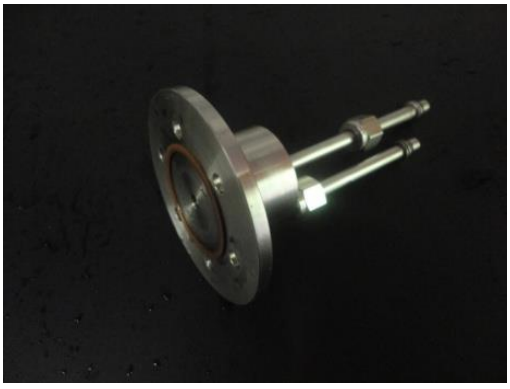

Figure 4. Picture of the manufactured injector.

3.2 Spray angle measurement

The experimental setup used for measuring the spray cone angle by photographic techniques consists of a support to fix the injector on the test bench and a digital camera. The pictures were obtained by a Sony DSC-F828 digital camera, with 8 megapixels of effective resolution, or 3264×2448 pixels. The support has a mark that serves to indicate a known length to be used as a reference to relate the number of pixels and the true length of the image, allowing determine the experimental values of the spray cone angles from the respective images.

Figure 5 shows the GUI (Graphical User Interface) developed in Matlab language by Vásquez (2011), especially written for this work to process spray images. The use of this GUI is relatively simple and the images can be treated in JPEG, TIFF or BMP formats.

After taking and selecting the appropriate images, the image processing is done with the GUI developed for this purpose. Finally, the experimental values of the spray cone angles of these images are registered. After data collection and treatment the experimental curves are obtained and compared to the theoretical data.

Figure 5. GUI for image processing.

4. RESULTS AND DISCUSSIONS

Figure 6 shows theoretical and experimental values of the mass flow rate in the primary and secondary chambers of the dual pressure swirl injector versus pressure injection.

Figure 7 shows theoretical and experimental values of the discharge coefficient in the primary and secondary chambers of the dual pressure swirl injector versus mass flow rate.

Figure 8 shows theoretical, semi-empirical and experimental values of the spray cone angle in the primary and secondary chambers of the dual pressure swirl injector versus mass flow rate.

The test fluids used in all experiments for the primary and secondary chambers were ethanol and water, respectively.

Figure 9 shows theoretical and experimental values of the mass flow rate in the primary chamber keeping fixed the mass flow rate of 40 g/s for the secondary chamber of the dual pressure swirl injector versus spray cone angle for simultaneous injection of ethanol/water or water/water.

As seen in Fig. 6, the mass flow rate of both chambers coincide with the analytical solution considering the viscous effects in the project conditions equals to 10 g/s and 40 g/s for primary and secondary chambers, respectively. In both chambers, note that smaller mass flow rates results in greater loss of angular momentum causing a slight discrepancy between the analytical solution and experimental data. The reverse also occurs.

As seen in Figs. 7, the discharge coefficients of both chambers of the dual pressure swirl injector had good agreement with the analytical solution considering the viscous effects for the entire operating range, except at low mass flow rates as mentioned above.

As seen in Fig. 8a, the Benjamin semi-empirical formulation provided the best estimated of the spray cone angle. The analytical solution considering the viscous effects has good agreement with experimental data, but was 16% lower in the project condition (10 g/s). This is expected, since the theoretical solution is a function only of the injector parameters and does not take into account the fluid properties and operating conditions. Another relevant fact is that analytical solution does not take into account the length of the vortex chamber and discharge orifice.

As seen in Fig. 8b, the analytical solution considering the viscous effects coincide with the experimental value in the project condition (40 g/s), but the experimental results did not follow the trend of the analytical solution, i.e., the spray cone angle should increase along with increasing mass flow rate. This behavior is due to the fact that secondary chamber presented was projected for a low pressure drop and therefore a fully developed spray was obtained only after

the project condition. The semi-empirical models could not be used for the secondary chamber, because they do not take into account the effect of the internal geometry of the flow of external injector.

As seen in Fig. 9, the analytical solution agreed with the experimental values. In tests, it was noticed that the interaction of both sprays leaves occurred when the primary chamber reached 8 g/s for both cases and it can be evidenced by the identical experimental values.

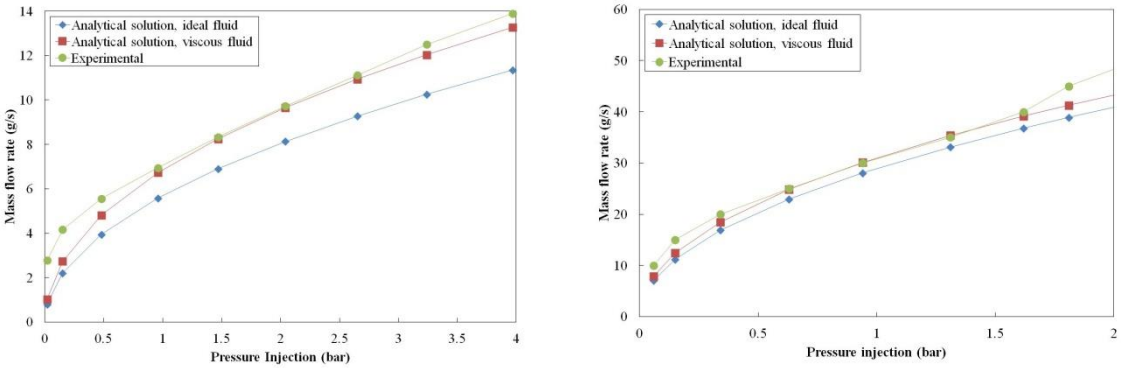

a) Primary chamber b) Secondary chamber

Figure 6. Theoretical and experimental values of the mass flow rate of ethanol versus pressure injection (gauge) in the primary chamber of the dual pressure swirl injector.

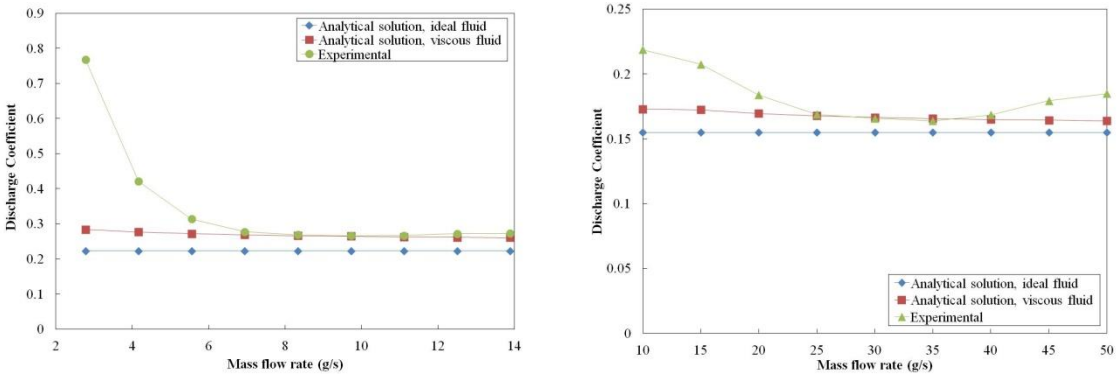

a) Primary chamber b) Secondary chamber

Figure 7. Theoretical and experimental values of the discharge coefficient versus mass flow rate in the primary chamber of the dual pressure swirl injector.

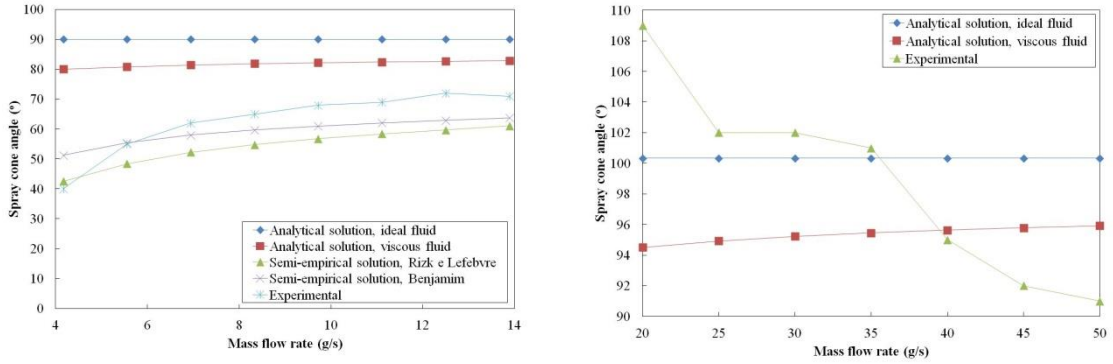

a) Primary chamber b) Secondary chamber

Figure 8. Theoretical, semi-empirical and experimental values of the spray cone angle of ethanol versus mass flow rate in the primary chamber of the dual pressure swirl injector.

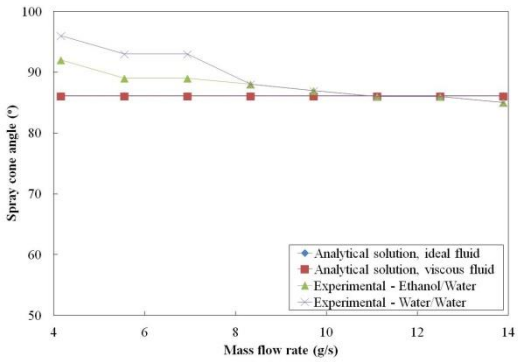

Figure 9. Theoretical and experimental values of the spray cone angle of ethanol versus mass flow rate in the primary chamber for simultaneous injection of ethanol/water or water/water.

5. CONCLUSIONS

Theoretical and semi-empirical spray cone angles for injection of ethanol and water in a dual pressure swirl injector were calculated and compared to experimental data. A graphical user interface was used to determine spray cone angles from spray images.

The discharge coefficients of both chambers of the dual pressure swirl injector had good agreement with the analytical solution considering the viscous effects for the entire operating range.

The semi-empirical models could not be used for the secondary chamber, because they do not take into account the effect of the internal geometry on the flow of external injector.

The Benjamin semi-empirical formulation provided the best estimates of spray cone angles for injection of ethanol in the injector primary chamber, thus indicating that both liquid physical properties and injector geometry are important to determination this parameter.

6. REFERENCES

Bayvel, L. and Orzechowski, Z., 1993. Liquid Atomization, Taylor & Francis, Washington, DC.

Bazarov, V.; Vigor, Y. and Puri, P., 2004. Design and dynamics of jet and swirl injectors, liquid rocket thrust chambers: aspects of modeling, analysis, and design. United States of America: American Institute of Aeronautics and Astronautics.

Borodin, V.A.; Dityakin, Yu.F.; Klyachko, L.A. and Yagodkin, V.L., 1967. Liquid Atomization, Mashinostroenie, Moscow.

Fischer, G.A.A., 2014. Injetores centrífugos duais e jato-centrífugos para aplicação em propulsão de foguetes, Master thesis, Instituto Nacional de Pesquisas Espaciais, São José dos Campos, SP, Brazil.

Giffen, E. and Muraszew, A., 1953. Atomization of Liquid Fuels, Chapman and Hall, London.

Khavkin, Y.I., 2004. Theory and practice swirl atomizers, Taylor & Francis, New York.

Kulagin, L.V. and Okhotnikov S.S., 1970. Combustion of Heavy Liquid Fuels, Mashinostroenie, Moscow.

Lefebvre, A.H., 1989. Atomization and Sprays, Hemisphere, New York.

Maia, F.F., 2012. Novo catalisador para decomposição de peróxido de hidrogênio em micropropulsores de satélites, Master Thesis, Instituto Nacional de Pesquisas Espaciais, São José dos Campos, SP, Brazil.

Matos, S.C., 2013. Ensaios em câmara de combustão com injetor centrífugo bipropelente líquido criogênico. Master thesis, Instituto Tecnológico de Aeronáutica, São José dos Campos, SP, Brazil.

Ortmann, J., and Lefebvre, A.H., 1985. Fuel Distributions from Pressure-swirl Atomizers, Journal Propulsion and Power, Vol. 1, No. 1, pp. 11-15.

Vásquez, R.A., 2011. Desenvolvimento de um injetor centrífugo dual para biocombustíveis líquidos, Master Thesis, Instituto Nacional de Pesquisas Espaciais, São José dos Campos, SP, Brazil.

Wernimont, E.J., 2006. Monopropellant hydrogen peroxide rocket system: optimum for small scale In: AIAA/ASME/SAE/JOINT PROPULSION CONFERENCE & EXHIBIT, n. 42, 9 – 12 de Jun de 2006, Sacramento CA. Proceedings... Sacramento: AIAA.

7. RESPONSIBILITY NOTICE

The authors are the only responsible for the printed material included in this paper.